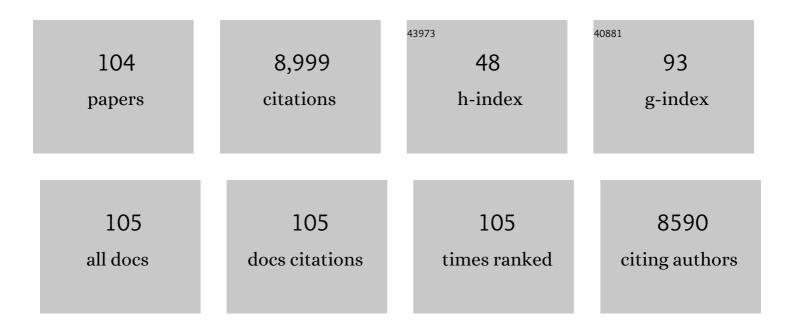


## List of Publications by Year in descending order

Source: https://exaly.com/author-pdf/8451052/publications.pdf Version: 2024-02-01



#	Article	IF	CITATIONS
1	Platinum single-atoms anchored covalent triazine framework for efficient photoreduction of CO2 to CH4. Chemical Engineering Journal, 2022, 427, 131018.	6.6	59
2	CuPd alloy decorated SnNb2O6 nanosheets as a multifunctional photocatalyst for semihydrogenation of phenylacetylene under visible light. Chemical Engineering Journal, 2022, 429, 132018.	6.6	12
3	Flowerlike BiOCl nanospheres fabricated by an in situ self-assembly strategy for efficiently enhancing photocatalysis. Journal of Colloid and Interface Science, 2022, 607, 423-430.	5.0	52
4	Surface functionalized Pt/SnNb2O6 nanosheets for visible-light-driven the precise hydrogenation of furfural to furfuryl alcohol. Journal of Energy Chemistry, 2022, 66, 566-575.	7.1	16
5	Enhanced photocatalytic benzyl alcohol oxidation over Bi4Ti3O12 ultrathin nanosheets. Journal of Colloid and Interface Science, 2022, 608, 2529-2538.	5.0	31
6	Facet-engineering palladium nanocrystals for remarkable photocatalytic dechlorination of polychlorinated biphenyls. Catalysis Science and Technology, 2022, 12, 192-200.	2.1	5
7	Visible-light-driven photocatalysis over nano-TiO2 with different morphologies: From morphology through active site to photocatalytic performance. Applied Surface Science, 2022, 580, 152262.	3.1	16
8	Surface synergetic effects of Pt clusters/monolayer Bi2MoO6 nanosheet for promoting the photocatalytic selective reduction of 4-nitrostyrene to 4-vinylaniline. Applied Catalysis B: Environmental, 2022, 304, 121010.	10.8	27
9	Oxygen vacancy enhanced visible light photocatalytic selective oxidation of benzylamine over ultrathin Pd/BiOCl nanosheets. Applied Catalysis B: Environmental, 2022, 305, 121032.	10.8	62
10	Dehydrated UiOâ€66(SH) <sub>2</sub> : The Zrâ^'O Cluster and Its Photocatalytic Role Mimicking the Biological Nitrogen Fixation. Angewandte Chemie - International Edition, 2022, 61, .	7.2	32
11	Synthesis of aluminum doped MIL-100(Fe) compounds for the one-pot photocatalytic conversion of cinnamaldehyde and benzyl alcohol to the corresponding alcohol and aldehyde under anaerobic conditions. Journal of Catalysis, 2022, 406, 184-192.	3.1	12
12	Covalent triazine-based frameworks confining cobalt single atoms for photocatalytic CO2 reduction and hydrogen production. Journal of Materials Science and Technology, 2022, 116, 41-49.	5.6	41
13	Functionalized UiO-66(Ce) for photocatalytic organic transformation: the role of active sites modulated by ligand functionalization. Catalysis Science and Technology, 2022, 12, 1812-1823.	2.1	29
14	Rational Design of Novel COF/MOF S-Scheme Heterojunction Photocatalyst for Boosting CO <sub>2</sub> Reduction at Gas–Solid Interface. ACS Applied Materials & Interfaces, 2022, 14, 24299-24308.	4.0	54
15	Ultrathin ZnTi-LDH nanosheets for photocatalytic aerobic oxidation of aniline based on coordination activation. Catalysis Science and Technology, 2021, 11, 162-170.	2.1	18
16	Visible-light-driven photocatalyst based upon metal-free covalent triazine-based frameworks for enhanced hydrogen production. Catalysis Science and Technology, 2021, 11, 1874-1880.	2.1	9
17	Direct Z-scheme copper cobaltite/covalent triazine-based framework heterojunction for efficient photocatalytic CO <sub>2</sub> reduction under visible light. Sustainable Energy and Fuels, 2021, 5, 732-739.	2.5	19
18	Selective hydrogenation of cinnamaldehyde to hydrocinnamaldehyde over Au-Pd/ultrathin SnNb2O6 nanosheets under visible light. Journal of Catalysis, 2021, 396, 374-386.	3.1	26

#	Article	IF	CITATIONS
19	Selective photocatalytic reduction CO2 to CH4 on ultrathin TiO2 nanosheet via coordination activation. Applied Catalysis B: Environmental, 2021, 288, 120000.	10.8	87
20	Band Gap Tuning of Covalent Triazineâ€Based Frameworks through Iron Doping for Visibleâ€Lightâ€Driven Photocatalytic Hydrogen Evolution. ChemSusChem, 2021, 14, 3850-3857.	3.6	19
21	Photocatalytic H2 evolution integrated with selective amines oxidation promoted by NiS2 decorated CdS nanosheets. Journal of Catalysis, 2021, 400, 347-354.	3.1	48
22	Rational construction of Ni(OH)2 nanoparticles on covalent triazine-based framework for artificial CO2 reduction. Journal of Colloid and Interface Science, 2021, 602, 23-31.	5.0	25
23	Unveiling the intermediates/pathways towards photocatalytic dechlorination of 3,3′,4,4′-trtrachlorobiphenyl over Pd /TiO2(B) nanosheets. Applied Catalysis B: Environmental, 2021, 298, 120526.	10.8	21
24	Constructing Nitrogen Self-Doped Covalent Triazine-Based Frameworks for Visible-Light-Driven Photocatalytic Conversion of CO <sub>2</sub> into CH <sub>4</sub> . ACS Sustainable Chemistry and Engineering, 2021, 9, 1333-1340.	3.2	43
25	Thiol-functionalized UiO-66 anchored atomically dispersed metal ions for the photocatalytic selective oxidation of benzyl alcohol. Chemical Communications, 2021, 57, 12151-12154.	2.2	9
26	Visible-light-driven H <sub>2</sub> production from heterostructured Zn <sub>0.5</sub> Cd <sub>0.5</sub> S–TiO <sub>2</sub> photocatalysts modified with reduced graphene oxides. New Journal of Chemistry, 2021, 45, 21415-21422.	1.4	0
27	Assembling Ultrafine SnO2 Nanoparticles on MIL-101(Cr) Octahedrons for Efficient Fuel Photocatalytic Denitrification. Molecules, 2021, 26, 7566.	1.7	13
28	Unsaturated Ni <sup>II</sup> Centers Mediated the Coordination Activation of Benzylamine for Enhancing Photocatalytic Activity over Ultrathin Ni MOF-74 Nanosheets. ACS Applied Materials & Interfaces, 2021, 13, 61286-61295.	4.0	23
29	Photocatalytic selective oxidation of benzyl alcohol over ZnTi-LDH: The effect of surface OH groups. Applied Catalysis B: Environmental, 2020, 260, 118185.	10.8	122
30	Pt decorated hierarchical Sb <sub>2</sub> WO <sub>6</sub> microspheres as a surface functionalized photocatalyst for the visible-light-driven reduction of nitrobenzene to aniline. Journal of Materials Chemistry A, 2020, 8, 18755-18766.	5.2	47
31	MOF-Derived Porous Fe2O3 Nanoparticles Coupled with CdS Quantum Dots for Degradation of Bisphenol A under Visible Light Irradiation. Nanomaterials, 2020, 10, 1701.	1.9	14
32	Pd nanoclusters/TiO2(B) nanosheets with surface defects toward rapid photocatalytic dehalogenation of polyhalogenated biphenyls under visible light. Applied Catalysis B: Environmental, 2020, 277, 119255.	10.8	58
33	Enhanced photocatalytic hydrogen evolution over monolayer HTi2NbO7 nanosheets with highly dispersed Pt nanoclusters. Applied Surface Science, 2020, 511, 145501.	3.1	15
34	Selective Photocatalytic Oxidation of Thioanisole on DUT-67(Zr) Mediated by Surface Coordination. Langmuir, 2020, 36, 2199-2208.	1.6	30
35	A facile in situ growth of CdS quantum dots on covalent triazine-based frameworks for photocatalytic H2 production. Journal of Alloys and Compounds, 2020, 833, 155057.	2.8	24
36	A Cobaltâ€Modified Covalent Triazineâ€Based Framework as an Efficient Cocatalyst for Visibleâ€Lightâ€Driven Photocatalytic CO <sub>2</sub> Reduction. ChemPlusChem, 2019, 84, 1149-1154.	1.3	40

#	Article	IF	CITATIONS
37	Photocatalytic synthesis of N-benzyleneamine from benzylamine on ultrathin BiOCl nanosheets under visible light. Journal of Catalysis, 2019, 380, 123-131.	3.1	70
38	Constructing surface synergistic effect in Cu-Cu2O hybrids and monolayer H1.4Ti1.65O4·H2O nanosheets for selective cinnamyl alcohol oxidation to cinnamaldehyde. Journal of Catalysis, 2019, 370, 461-469.	3.1	17
39	Preparation of monolayer HSr <sub>2</sub> Nb <sub>3</sub> O <sub>10</sub> nanosheets for photocatalytic hydrogen evolution. Dalton Transactions, 2019, 48, 11136-11141.	1.6	11
40	Constructing a novel family of halogen-doped covalent triazine-based frameworks as efficient metal-free photocatalysts for hydrogen production. Nanoscale Advances, 2019, 1, 2674-2680.	2.2	41
41	Functionalized MIL-68(In) for the photocatalytic treatment of Cr(VI)-containing simulation wastewater: Electronic effects of ligand substitution. Applied Surface Science, 2019, 464, 396-403.	3.1	60
42	Hierarchical Bi2MoO6 spheres in situ assembled by monolayer nanosheets toward photocatalytic selective oxidation of benzyl alcohol. Applied Catalysis B: Environmental, 2019, 243, 10-18.	10.8	201
43	Photocatalytic oxidation of aniline over MO/TiO2 (M = Mg, Ca, Sr, Ba) under visible light irradiation. Catalysis Today, 2019, 335, 312-318.	2.2	14
44	Ultrasmall NiS decorated HNb3O8 nanosheeets as highly efficient photocatalyst for H2 evolution reaction. Catalysis Today, 2019, 330, 195-202.	2.2	46
45	Phase transformation synthesis of a new Bi2SeO5 flower-like microsphere for efficiently photocatalytic degradation of organic pollutants. Catalysis Today, 2019, 327, 357-365.	2.2	10
46	MoS <sub>2</sub> Quantum Dotsâ€Modified Covalent Triazineâ€Based Frameworks for Enhanced Photocatalytic Hydrogen Evolution. ChemSusChem, 2018, 11, 1108-1113.	3.6	80
47	Synthesis of nitrosobenzene via photocatalytic oxidation of aniline over MgO/TiO2 under visible light irradiation. Applied Surface Science, 2018, 440, 1269-1276.	3.1	21
48	Rapid water disinfection over a Ag/AgBr/covalent triazine-based framework composite under visible light. Dalton Transactions, 2018, 47, 7077-7082.	1.6	24
49	One-pot synthesis of secondary amine via photoalkylation of nitroarenes with benzyl alcohol over Pd/monolayer H1.07Ti1.73O4A·H2O nanosheets. Journal of Catalysis, 2018, 361, 105-115.	3.1	37
50	Facile in situ growth of highly dispersed palladium on phosphotungstic-acid-encapsulated MIL-100(Fe) for the degradation of pharmaceuticals and personal care products under visible light. Nano Research, 2018, 11, 1109-1123.	5.8	44
51	Photocatalytic hydrogen evolution over monolayer H1.07Ti1.73O4·H2O nanosheets: Roles of metal defects and greatly enhanced performances. Applied Catalysis B: Environmental, 2018, 221, 473-481.	10.8	56
52	Highly selective oxidation of furfuryl alcohol over monolayer titanate nanosheet under visible light irradiation. Applied Catalysis B: Environmental, 2018, 224, 394-403.	10.8	47
53	The cooperation effect in the Au–Pd/LDH for promoting photocatalytic selective oxidation of benzyl alcohol. Catalysis Science and Technology, 2018, 8, 268-275.	2.1	87
54	Efficient Visible-Light-Driven Photocatalytic Hydrogen Evolution on Phosphorus-Doped Covalent Triazine-Based Frameworks. ACS Applied Materials & Interfaces, 2018, 10, 41415-41421.	4.0	82

#	Article	IF	CITATIONS
55	Selective Photocatalytic Synthesis of Haloanilines from Halonitrobenzenes over Multifunctional AuPt/Monolayer Titanate Nanosheet. ACS Catalysis, 2018, 8, 9656-9664.	5.5	41
56	MIL-68(Fe) as an efficient visible-light-driven photocatalyst for the treatment of a simulated waste-water contain Cr(VI) and Malachite Green. Applied Catalysis B: Environmental, 2017, 206, 9-15.	10.8	145
57	Engineering a highly dispersed co-catalyst on a few-layered catalyst for efficient photocatalytic H <sub>2</sub> evolution: a case study of Ni(OH) <sub>2</sub> /HNb <sub>3</sub> O <sub>8</sub> nanocomposites. Catalysis Science and Technology, 2017, 7, 5662-5669.	2.1	29
58	A hybrid of CdS/HCa <sub>2</sub> Nb <sub>3</sub> O <sub>10</sub> ultrathin nanosheets for promoting photocatalytic hydrogen evolution. Dalton Transactions, 2017, 46, 13935-13942.	1.6	19
59	An unsaturated metal site-promoted approach to construct strongly coupled noble metal/HNb <sub>3</sub> O <sub>8</sub> nanosheets for efficient thermo/photo-catalytic reduction. Nanoscale, 2017, 9, 14654-14663.	2.8	30
60	Enhanced Photocatalytic Fuel Denitrification over TiO2/α-Fe2O3 Nanocomposites under Visible Light Irradiation. Scientific Reports, 2017, 7, 7858.	1.6	34
61	Development and photocatalytic mechanism of monolayer Bi <sub>2</sub> MoO <sub>6</sub> nanosheets for the selective oxidation of benzylic alcohols. Chemical Communications, 2017, 53, 8604-8607.	2.2	91
62	SnS2 nanoplates/SnO2 nanotubes composites as efficient visible light-driven photocatalysts for Cr(VI) reduction. Research on Chemical Intermediates, 2017, 43, 5217-5228.	1.3	12
63	A Pd/Monolayer Titanate Nanosheet with Surface Synergetic Effects for Precise Synthesis of Cyclohexanones. ACS Catalysis, 2017, 7, 8664-8674.	5.5	69
64	HNbxTa1-xWO6 monolayer nanosheets solid solutions: Tunable energy band structures and highly enhanced photocatalytic performances for hydrogen evolution. Applied Catalysis B: Environmental, 2017, 203, 798-806.	10.8	20
65	Highly efficient photocatalytic H2 evolution over MoS2/CdS-TiO2 nanofibers prepared by an electrospinning mediated photodeposition method. Applied Catalysis B: Environmental, 2017, 202, 374-380.	10.8	189
66	Constructing a MoS2 QDs/CdS Core/Shell Flowerlike Nanosphere Hierarchical Heterostructure for the Enhanced Stability and Photocatalytic Activity. Molecules, 2016, 21, 213.	1.7	32
67	Insights into the role of Cu in promoting photocatalytic hydrogen production over ultrathin HNb3O8 nanosheets. Journal of Catalysis, 2016, 342, 98-104.	3.1	51
68	Effective photo-reduction to deposit Pt nanoparticles on MIL-100(Fe) for visible-light-induced hydrogen evolution. New Journal of Chemistry, 2016, 40, 9170-9175.	1.4	65
69	Photocatalytic reduction of CO <sub>2</sub> with H <sub>2</sub> O to CH <sub>4</sub> over ultrathin SnNb <sub>2</sub> O <sub>6</sub> 2D nanosheets under visible light irradiation. Green Chemistry, 2016, 18, 1355-1363.	4.6	129
70	Covalent Triazineâ€Based Frameworks as Visible Light Photocatalysts for the Splitting of Water. Macromolecular Rapid Communications, 2015, 36, 1799-1805.	2.0	239
71	Macromol. Rapid Commun. 20/2015. Macromolecular Rapid Communications, 2015, 36, 1798-1798.	2.0	0
72	Strategies for engineering metal-organic frameworks as efficient photocatalysts. Chinese Journal of Catalysis, 2015, 36, 2071-2088.	6.9	113

5

#	Article	IF	CITATIONS
73	Fabrication of hierarchical CdS nanosphere via one-pot process for photocatalytic water splitting. Journal of Nanoparticle Research, 2015, 17, 1.	0.8	8
74	MIL-53(Fe) as a highly efficient bifunctional photocatalyst for the simultaneous reduction of Cr(VI) and oxidation of dyes. Journal of Hazardous Materials, 2015, 287, 364-372.	6.5	555
75	A Clean and General Strategy To Decorate a Titanium Metal–Organic Framework with Noble-Metal Nanoparticles for Versatile Photocatalytic Applications. Inorganic Chemistry, 2015, 54, 1191-1193.	1.9	157
76	An architecture of CdS/H <sub>2</sub> Ti <sub>5</sub> O <sub>11</sub> ultrathin nanobelt for photocatalytic hydrogenation of 4-nitroaniline with highly efficient performance. Journal of Materials Chemistry A, 2015, 3, 6935-6942.	5.2	26
77	Preparation of MIL-53(Fe)-Reduced Graphene Oxide Nanocomposites by a Simple Self-Assembly Strategy for Increasing Interfacial Contact: Efficient Visible-Light Photocatalysts. ACS Applied Materials & Interfaces, 2015, 7, 9507-9515.	4.0	239
78	An efficient cocatalyst of defect-decorated MoS <sub>2</sub> ultrathin nanoplates for the promotion of photocatalytic hydrogen evolution over CdS nanocrystal. Journal of Materials Chemistry A, 2015, 3, 12631-12635.	5.2	128
79	A simple strategy for fabrication of Pd@MIL-100(Fe) nanocomposite as a visible-light-driven photocatalyst for the treatment of pharmaceuticals and personal care products (PPCPs). Applied Catalysis B: Environmental, 2015, 176-177, 240-248.	10.8	227
80	Multifunctional polyoxometalates encapsulated in MIL-100(Fe): highly efficient photocatalysts for selective transformation under visible light. Dalton Transactions, 2015, 44, 18227-18236.	1.6	115
81	Au and Pt co-loaded g-C3N4 nanosheets for enhanced photocatalytic hydrogen production under visible light irradiation. Applied Surface Science, 2015, 358, 304-312.	3.1	134
82	M@MIL-100(Fe) (M = Au, Pd, Pt) nanocomposites fabricated by a facile photodeposition process: Efficient visible-light photocatalysts for redox reactions in water. Nano Research, 2015, 8, 3237-3249.	5.8	164
83	Ultrathin HNbWO <sub>6</sub> nanosheets: facile synthesis and enhanced hydrogen evolution performance from photocatalytic water splitting. Chemical Communications, 2015, 51, 15125-15128.	2.2	49
84	Ultrathin HNb <sub>3</sub> O <sub>8</sub> nanosheet: an efficient photocatalyst for the hydrogen production. Journal of Materials Chemistry A, 2015, 3, 20627-20632.	5.2	79
85	Noble-metal-free MoS2 co-catalyst decorated UiO-66/CdS hybrids for efficient photocatalytic H2 production. Applied Catalysis B: Environmental, 2015, 166-167, 445-453.	10.8	283
86	Electronic effects of ligand substitution on metal–organic framework photocatalysts: the case study of UiO-66. Physical Chemistry Chemical Physics, 2015, 17, 117-121.	1.3	233
87	Efficient synthesis of monolayer carbon nitride 2D nanosheet with tunable concentration and enhanced visible-light photocatalytic activities. Applied Catalysis B: Environmental, 2015, 163, 135-142.	10.8	487
88	Monolayer HNb <sub>3</sub> O <sub>8</sub> for Selective Photocatalytic Oxidation of Benzylic Alcohols with Visible Light Response. Angewandte Chemie - International Edition, 2014, 53, 2951-2955.	7.2	201
89	Enhanced photocatalytic hydrogen production activity via dual modification of MOF and reduced graphene oxide on CdS. Chemical Communications, 2014, 50, 8533.	2.2	212
90	Novel hierarchical architectures of Sb2WO6: template-free hydrothermal synthesis and photocatalytic reduction property for azo compound. Journal of Nanoparticle Research, 2013, 15, 1.	0.8	22

#	Article	IF	CITATIONS
91	Highly dispersed palladium nanoparticles anchored on UiO-66(NH2) metal-organic framework as a reusable and dual functional visible-light-driven photocatalyst. Nanoscale, 2013, 5, 9374.	2.8	417
92	CdS-decorated UiO–66(NH2) nanocomposites fabricated by a facile photodeposition process: an efficient and stable visible-light-driven photocatalyst for selective oxidation of alcohols. Journal of Materials Chemistry A, 2013, 1, 11473.	5.2	261
93	A new insight into the photocatalytic reduction of 4-nitroaniline to p-phenylenediamine in the presence of alcohols. Applied Catalysis B: Environmental, 2013, 130-131, 163-167.	10.8	51
94	Highly efficient visible-light-induced photocatalytic hydrogenation of nitrobenzene to aniline in water. RSC Advances, 2013, 3, 10894.	1.7	33
95	Mechanistic insight into the photocatalytic hydrogenation of 4-nitroaniline over band-gap-tunable CdS photocatalysts. Physical Chemistry Chemical Physics, 2013, 15, 19422.	1.3	32
96	Multifunctional NH2-mediated zirconium metal–organic framework as an efficient visible-light-driven photocatalyst for selective oxidation of alcohols and reduction of aqueous Cr(vi). Dalton Transactions, 2013, 42, 13649.	1.6	373
97	Rapid template-free synthesis and photocatalytic performance of visible light-activated SnNb2O6nanosheets. Journal of Materials Chemistry, 2012, 22, 2670-2678.	6.7	103
98	Molecular recognitive photocatalytic degradation of various cationic pollutants by the selective adsorption on visible light-driven SnNb2O6 nanosheet photocatalyst. Applied Catalysis B: Environmental, 2012, 125, 103-110.	10.8	111
99	A simple and highly efficient route for the preparation of p-phenylenediamine by reducing 4-nitroaniline over commercial CdS visible light-driven photocatalyst in water. Green Chemistry, 2012, 14, 1705.	4.6	85
100	Efficient visible-light-induced photocatalytic reduction of 4-nitroaniline to p-phenylenediamine over nanocrystalline PbBi2Nb2O9. Journal of Catalysis, 2012, 290, 13-17.	3.1	62
101	P NMR studies on the ligand dissociation of trinuclear molybdenum cluster compounds. Chinese Journal of Chemistry, 2010, 21, 1174-1177.	2.6	2
102	Simple solvothermal routes to synthesize nanocrystalline Bi2MoO6 photocatalysts with different morphologies. Acta Materialia, 2007, 55, 4699-4705.	3.8	217
103	Characterization and photocatalytic mechanism of nanosized CdS coupled TiO2 nanocrystals under visible light irradiation. Journal of Molecular Catalysis A, 2006, 244, 25-32.	4.8	415
104	A General inâ€situ Hydrothermal Rolling-Up Formation of One-Dimensional, Single-Crystalline Lead Telluride Nanostructures. Small, 2005, 1, 349-354.	5.2	75